



EPA Public Access

Author manuscript

Chemosphere. Author manuscript; available in PMC 2020 June 19.

About author manuscripts

Submit a manuscript

Published in final edited form as:

Chemosphere. 2016 October ; 161: 382–389. doi:10.1016/j.chemosphere.2016.06.078.

Anaerobic biodegradation of soybean biodiesel and diesel blends under sulfate-reducing conditions

Shuyun Wu^a, Mohamad H. Yassine^b, Makram T. Suidan^c, Albert D. Venosa^d

^aDepartment of Biomedical, Chemical, and Environmental Engineering, University of Cincinnati, Cincinnati, OH 45220, United States

^bDepartment of Mathematics and Natural Sciences, College of Arts and Sciences, Gulf University for Science and Technology, Hawally 32093, Kuwait

^cFaculty of Engineering and Architecture, American University of Beirut, Beirut, Lebanon

^dU.S. Environmental Protection Agency (retired), National Risk Management Research Laboratory, 26 W. Martin Luther King Drive, Cincinnati, OH 45268, United States

Abstract

Biotransformation of soybean biodiesel and its biodiesel/petrodiesel blends were investigated under sulfate-reducing conditions. Three blends of biodiesel, B100, B50, and B0, were treated using microbial cultures pre-acclimated to B100 (biodiesel only) and B80 (80% biodiesel and 20% petrodiesel). Results indicate that the biodiesel could be effectively biodegraded in the presence or absence of petrodiesel, whereas petrodiesel could not be biodegraded at all under sulfate-reducing conditions. The kinetics of biodegradation of individual Fatty Acid Methyl Ester (FAME) compounds and their accompanying sulfate-reduction rates were studied using a serum bottle test. As for the biodegradation of individual FAME compounds, the biodegradation rates for the saturated FAMEs decreased with increasing carbon chain length. For unsaturated FAMEs, biodegradation rates increased with increasing number of double bonds. The presence of petrodiesel had a greater effect on the rate of biodegradation of biodiesel than on the extent of removal.

Keywords

Biodiesel; FAMEs; Alkane; Anaerobic biodegradation; Sulfate-reduction

1. Introduction

Biodiesel is a mixture of monoalkyl esters of long-chain fatty acids derived from transesterification of vegetable oils or animal lipids. It has been attracting great interest as an alternative fuel because of its potential as a renewable, easily biodegradable energy source that can contribute to decreased greenhouse gas (GHG) emissions. Since the passage of the Energy Policy Act of 2005, the annual production of biodiesel increased more than 18-fold

Appendix A. Supplementary data

The following is the supplementary data related to this article: S1: Schematic of chemostat.

by 2013. The Energy Independence and Security Act of 2007 increased the volume of renewable fuel required to be blended into transportation fuel from 9 billion gallons in 2008 to 36 billion gallons by 2022. With the increasing usage of biodiesel, a thorough understanding of its fate in the environment is required since biofuels pose similar environmental risks as fossil fuels when released to the environment. However, the susceptibility of these fuel blends to biological degradation is insufficiently understood and the reported studies about the biodegradation of biodiesel blends have principally focused on aerobic processes (DeMello et al., 2007, Owsianiak et al., 2009, Yassine et al., 2013), whereas the anaerobic conditions prevail in subsurface environments where unintended fuel releases frequently occur. Biodiesel is often used in the form of fuel blends with petrodiesel and the physicochemical properties of their mixtures are more indeterminate and differ from those of the neat fuels when they are blended together. Therefore, understanding the biodegradation patterns of biodiesel and petrodiesel blends under anaerobic conditions is very important. Recent attempts to investigate the biodegradation of biodiesel and petrodiesel blends under anaerobic conditions have been very modest (Aktas et al., 2010, Sørensen et al., 2011, Wu et al., 2015). Aktas et al. (2010) evaluated anaerobic biodegradation of biodiesel by five anaerobic inocula and found that biodiesel could be easily hydrolyzed and converted to a variety of fatty acid intermediates within one month under sulfate reduction and methanogenic conditions. Sørensen et al., 2011 reported that the activity of all three groups of anaerobes (methanogens, sulfate- and nitrate-reducers) was stimulated by the presence of biodiesel. Wu et al. (2015) investigated the biodegradation of biodiesel and petrodiesel blends under methanogenic conditions and observed that when biodiesel was blended with low concentrations of petrodiesel, the petrodiesel did not impact the biodegradation of biodiesel much. Significant effects on the biodegradation rate and extent of transformation started appearing when petrodiesel and biodiesel were present in equal volumetric proportions (B50). There are no reported studies of the anaerobic biodegradation of biodiesel under iron reducing conditions.

Petrodiesel is composed mostly of saturated and aromatic petroleum hydrocarbons. It exhibits low biochemical reactivity and for many decades was thought to undergo biodegradation only in the presence of molecular oxygen. Biodegradation of petrodiesel under strictly anaerobic conditions has been frequently reported in the past decade (Rueter et al., 1994; Widdel and Rabus, 2001, Wentzel et al., 2007). Boopathy (2004) evaluated the biodegradation of petrodiesel under various anaerobic conditions in soil columns and found that the highest petrodiesel biodegradation rate was under mixed electron acceptor conditions followed by sulfate-reducing, nitrate-reducing, and finally methanogenic conditions. However, even under optimum conditions, anaerobic biodegradation was reported to require in excess of 310 days to achieve 81% transformation of petrodiesel fuel. Mukherji et al. (2004) reported that the maximum degradation of petrodiesel by a culture isolated from deep-sea sediment was only 18% over 50 days under anoxic nitrate-reducing conditions. It appears that the biodegradation of petrodiesel under anaerobic conditions mostly occurs under sulfate-reducing conditions either after long exposure times or when present in low environmental concentrations. Some studies have shown that adding biodiesel to the fuel blends could promote and enhance the biodegradation of petrodiesel under aerobic conditions (Miller and Mudge., 1997, Zhang et al., 1998, Pasqualino et al., 2006,

DeMello et al., 2007 and Yassine et al., 2013). Miller and Mudge (1997) suggested that this enhancement was achieved through co-solubilization while Zhang et al. (1998) and Pasqualino et al. (2006) claimed it was achieved by co-metabolism. Whether biodiesel blending would promote the biodegradation of petrodiesel under anaerobic conditions is still unknown, and the biodegradation of biodiesel/petrodiesel blends under anaerobic conditions has been rarely investigated to date. The objective of this study was to investigate anaerobic biodegradation of soybean biodiesel and petrodiesel blends in a sulfate-reducing environment, which is a prevalent condition in anaerobic sediments. Serum Bottle Reactor (SBR) tests of pure unblended biodiesel (B100), pure unblended petrodiesel (B0), and B50 were conducted to determine the anaerobic biodegradation kinetics of individual FAME compounds in biodiesel and the associated sulfate utilization rate.

2. Materials and methods

2.1. Chemicals

Unblended soybean biodiesel (B100) was purchased from Peter Cramer North America (Cincinnati, OH) with FAMES mole fractions of 0.145 C16:0-methyl ester (ME), 0.055 C18:0-ME, 0.206 C18:1-ME, 0.518 C18:2-ME, and 0.0759 C18:3-ME. Low-sulfur petrodiesel (B0) was purchased from a local BP petrodiesel station (Cincinnati, OH) with a mole fraction of 0.165 nC10-nC23 n-alkanes. B50 fuel blend was blended in our laboratory by volumetric splash mixing. Palmitic acid methyl ester (99%), palmitoleic acid methyl ester (99%), stearic acid methyl ester (99%), oleic acid methyl ester (99%), linoleic acid methyl ester (99%), linolenic acid methyl ester (99%), and n-alkanes standard mixture (nC10-nC30), were all purchased from Sigma Aldrich (USA).

2.2. Culture acclimation

Two 12-L laboratory-scale continuous flow stirred-tank reactors (CSTR) with a solids retention time of 40 days were used to enrich for bacterial cultures capable of biodegrading biodiesel under sulfate reducing conditions at room temperature 22 °C. The cultures were obtained from an anaerobic digester at a local wastewater treatment plant in Cincinnati, OH. A schematic of the bioreactor is provided in Fig. S1 in the supplementary material section. 1.4 g/L organic feed of B100 (biodiesel only) and B80 (80% biodiesel and 20% petrodiesel) were respectively delivered to the bioreactors through Hamilton syringe pumps. It was not possible to enrich for B50 due to the inhibitory effect of petrodiesel. At the onset of this study sodium and ammonium sulfate were added to the nutrient solution to convert the redox conditions from methanogenic to sulfate-reducing. Sodium molybdate ($\text{Na}_2\text{MoO}_4 \cdot 2\text{H}_2\text{O}$), which inhibits sulfate-reducing bacteria (Pareek et al., 2000), was not added to the nutrient solution. In a sulfate-reducing environment, sulfide is produced via the reduction of sulfate. High concentrations of sulfide have been reported to inhibit sulfate-reducing microorganisms (Maillacheruvu et al., 1993). To minimize the potential for inhibition and to avoid sequestration of heavy metals in the nutrient solution via sulfide precipitation, excess ferrous iron in the form of $\text{FeCl}_2 \cdot 4\text{H}_2\text{O}$ was added to the nutrient feed. The bioreactors received a separate combined feed of essential nutrients solution and vitamins minimal medium as the following final concentrations: 1351 mg/L Na_2SO_4 , 7691 mg/L $\text{FeSO}_4 \cdot 7\text{H}_2\text{O}$, 450 mg/L NH_4SO_4 , 119 mg/L $\text{MgSO}_4 \cdot 6\text{H}_2\text{O}$, 70.8 mg/L $\text{CaCl}_2 \cdot 2\text{H}_2\text{O}$, 2666

mg/L FeCl₂·4H₂O, 9.59 mg/L CuSO₄·5H₂O, 13 mg/L MnSO₄·H₂O, 10.5 mg/L ZnCl₂, 9.16 mg/L CoCl₂·6H₂O, 0.64 mg/L B(OH)₃, 9.58 mg/L NiCl₂·6H₂O, 0.24 mg/L 4-aminobenzoic acid (99%), 0.096 mg/L biotin, 0.0048 mg/L cyanocobalamin, 0.096 mg/L, folic acid dihydrate (99%), 0.24 mg/L nicotinic acid (98%), 0.24 mg/L pantothenic acid Ca-salt hydrate (98%), 0.48 mg/L pyridoxine hydrochloride (98%), 0.24 mg/L riboflavin (98%), 0.24 mg/L thiamine hydrochloride (99%), 0.24 mg/L thiocetic acid (98%). The same nutrients growth medium was used in the batch experiments. A buffer solution containing 3250 mg/L Na₂CO₃, 3250 mg/L K₂CO₃, 208 mg/L KH₂PO₄ provided a strong buffering capacity to maintain the pH in the bioreactor at 7.0 ± 0.2. The flow rate of the nutrient and buffer solutions was monitored on a daily basis. Water quality variables including pH, target analytes in effluent including FAMES and n-alkanes, volatile fatty acids (VFAs), influent sulfate, effluent sulfate, total and volatile suspended solids (TSS/VSS), and effluent chemical oxygen demand (COD) were monitored routinely. The gas meter showed no gas production, because the carbon dioxide produced by sulfate reduction remained in the aqueous phase, in equilibrium, with carbonate and bicarbonate. Methane was detected in the headspace of the chemostat, however, the amount produced was very small and difficult to quantify. Gas composition was analyzed weekly to check for leaks (Oxygen composition <1%).

2.3. Analytical methods

For the batch experiments, every sampling event consisted of randomly selecting triplicate bottles of each experimental treatment. At each sampling event, a 0.5 ml of the headspace gas was withdrawn by a gastight Vici Precision Sampling Syringe (Baton Rouge, LA) Gas composition analyzed using an HP5890 Series II Gas Chromatograph (GC) (Hewlett Packard, Wilmington, Delaware) equipped with a thermal conductivity detector (TCD) using an HP 10 ft molecular sieve (BX-45/60 mesh) and an HP 6 ft HAYESEPQ 80/100 column (Supelco, Bellefonte, Pennsylvania). Reference standard gas (Wright Brothers, Cincinnati, Ohio) was used for the calibration of the instrument. The standard gas volume composition were as follows: 35% CO₂; 1% O₂; 4% N₂, 60% CH₄, and the quantitation limit was 0.01%. After gas composition analysis, 1 ml of the bottle contents was withdrawn and filtered through a 0.45 µm filter, 0.5 ml filtered liquid was diluted 20 times with deionized water for sulfate analysis. A 1 ml diluted sample was analyzed using an ion chromatograph (dx 500 system DIONEX Corporation, Sunnyvale, CA), equipped with an anion guard column DIONEX AG 16 4 mm, and anion separator column–DIONEX AS 16 4 mm (DIONEX Corporation, Sunnyvale, CA). The quantitation limit was 1 mg/L for sulfate. The remaining 49 ml was completely liquid-liquid extracted with 50 ml dichloromethane. 50 µl standard surrogate solution of C16:1-ME and deuterated nC16 in acetone were spiked during the extraction. The surrogate recoveries of all extractions ranged from 80 to 120%, and were used to ensure that extraction recoveries were within the permissible limits of EPA method 8000. The extracts were filtered through anhydrous sodium sulfate to remove any water and stored at -20 °C until analysis using HP Agilent 5890 II Gas Chromatograph (GC) equipped with an HP-INNOWAX capillary column (30 m long, 0.25 mm i.d., 0.25 µm film thickness), and an HP Agilent 5971 Mass Spectrometer Detector (MSD). At the time of analysis, the extracts were aliquoted in 1 mL GC vials and spiked with 10 µL of an internal standard solution containing C11:0-ME, C13:0-ME, deuterated nC10, and deuterated nC20 in DCM.

The flow rate of the Helium carrier gas was 1 mL/min. Both the inlet and detector interface temperatures were held at 320 °C, the former was operated in splitless mode. Oven temperature program was as follows: hold at 35 °C for 3 min, ramp at 5 °C/min to 250 °C, and hold at 250 °C for 5 min. The quantitation limits were in the range of 3–25 µg/L for FAMES and Alkanes. TSS and VSS in the bioreactors were determined in accordance to EPA methods 160.2 and 160.4, respectively. The pH was measured using an Orion Model 720A pH meter (Orion Research, Boston, Massachusetts). COD was measured using Hach method 8000 on a Hach DR/200 Spectrophotometer (Hach, Loveland, Colorado). VFAs were measured using HP Agilent 6890 II GC equipped with a flame ionization detector (FID) using a 2 mm i.d. 1.83 m glass column packed with 4% Carbowax on an 80/120 Carbowax B-DA (Supelco, Bellefonte, Pennsylvania). The quantitation limit for VFAs was 0.5 mg/L.

2.4. Serum bottle reactor tests

After an acclimation period of six months, biodiesel removal exceeding 95% was achieved in the chemostats. The stoichiometry for sulfate consumption was 4.1 mg sulfate/mg biodiesel. The chemostats achieved steady state, i.e., several consecutive measurements revealed consistently low effluent concentrations of the FAMES (<0.5 mg/L), VFAs (<4 mg/L) and effluent COD (<40 mg/L). Two batches of SBR tests were carried out using biomass collected from the bioreactor feeding B100 and bioreactor feeding B80, with an observed solids concentration of 169 ± 15 mg VSS/L for culture B100 and 186 ± 18 mg VSS/L for culture B80 respectively. The SBR tests followed the procedure outlined by Gupta et al. (1996). Sterilized and surface-deactivated 60 ml serum bottles were placed in an anaerobic chamber (model 1024 Forma Scientific, Marietta, Ohio). Prepared nutrient solution was purged for 5 h with nitrogen gas and stirred inside the anaerobic system for 2 days to remove any trace oxygen in the solution. Gas composition inside the anaerobic chamber was monitored using GC-TCD to ensure strict anaerobic conditions during the whole process ($O_2 < 0.02\%$). Inside the chamber, each 60 ml bottle was filled with 25 ml of the effluent from the reactors (which contained the anaerobic biomass), 25 ml of deoxygenated nutrient and buffer solution, and 10 ml N_2 headspace. After addition of the various solutions, the initial pH was 7.5 ± 0.1 . Then each serum bottle was sealed with rubber lined PTFE[®] septa and aluminum caps. 15 µl of 1 of 3 different blended fractions of petrodiesel and biodiesel (B100, B50 and B0) was spiked into each serum bottle. The sulfate concentration in the solution was sufficient to complete the biodegradation of approximately twice the amount of oil added. All serum bottles were then placed in a rotary tumbler operated at a nominal speed of 20–25 rpm. In the case of B100 treatment, 11 sampling events took place at 0, 1, 2, 3, 4, 5, 7, 9, 12, 15, and 19 days. In the case of B50 treatment, 12 sampling events took place at 0, 1, 2, 3, 4, 5, 7, 10, 14, 19, 24, and 30 days. In the case of B0 treatment, 9 sampling events took place at 0, 1, 3, 6, 10, 14, 19, 24, and 30 days. To quantify abiotic substrate losses, Autoclaved Microbial Control (AMC) samples were prepared according to the same procedure except the effluent was autoclaved at 121 °C for 60 min and they were sampled at 9 and 19 days for B100 treatment, 15 and 30 days for B50 and B0 treatments. All the experiments were carried out at room temperature 22 °C.

3. Results and discussion

3.1. Sulfate utilization

Sulfate was added to the serum bottles in excess of what was theoretically needed to ensure the potential for complete degradation of the substrate, as shown in Fig. 1. The biodegradation first order rate constants for sulfate consumption were estimated by nonlinear least-squares regression using SigmaPlot 11 (systatsoftware. Inc., CA) by fitting the sulfate data to exponential decay equation (Aeckersberg et al., 1998),

Where S_0 is the excess sulfate; S^* is the ultimate degraded sulfate; b is the pseudo-first order rate constant. For the B100 and B50 treatments with culture pre-acclimated to B100 (Culture B100), the pseudo-first rate constants were $0.18 \pm 0.03 \text{ d}^{-1}$ for B100 (open circle symbols in Fig. 1A) and $0.20 \pm 0.04 \text{ d}^{-1}$ for B50 (open triangle symbols in Fig. 1A). The rate constant was slightly higher for B50, although the initial concentration of FAMES in B100 was twice the concentration in B50. When the total mass and rate of sulfate utilized was compared to the total mass and rate of FAMES degraded for B100, the ratio of sulfate consumption to FAMES utilization was found to be 4.3 mg sulfate/mg FAMES, corresponding to 1.4 sulfate/COD ratio, which is in accordance with the chemostat sulfate utilization and slightly lower than the theoretical value of 1.5. Trace amounts of methane were detected in the headspace at the end of test, indicating that trace amount of biodiesel biodegraded via methanogenic activity. Another series of SBR tests were run with the biomass pre-acclimated to B80. For the treatment of B100 and B50, the pseudo-first order rate constants of sulfate utilization were respectively $0.06 \pm 0.02 \text{ d}^{-1}$ (open circle symbols in Fig. 1B) and $0.08 \pm 0.03 \text{ d}^{-1}$ (open triangle symbols in Fig. 1B).

These results show that when using culture B80, the sulfate utilization rate was decreased by 36% for the B100 substrate treatment and 43% for the B50 treatment compared to using culture B100. This decrease in sulfate utilization rates when changing the biomass pre-acclimation from B100 to B80 was greater than the 20% difference in biodiesel in the reactor feed to the two chemostats, which suggests that the activity of the culture could have been inhibited by the presence of petrodiesel in the B80 acclimated culture feed. Yassine et al. (2012) examined the Microtox™ toxicity of the Water Accommodated Fraction (WAF) of six soybean biodiesel and petrodiesel blends at different oil loads and observed that when dilutions exceeded 1:1000, the toxicity of the WAF was decreased when the fraction of biodiesel increased in the blends. Hence, B80 becomes more toxic than B100. In fact, analysis of the petrodiesel fraction in the effluent showed that it did not degrade and instead accumulated in the chemostat. Consequently, the microorganisms in the reactor fed on B80 were subjected to the toxicity of petrodiesel in B80 blends and this seems to have resulted in lower microbial activity. There was no decline in sulfate concentration in the B0 substrate treatment using culture B100, culture B80, and KCs indicating that no petrodiesel was degraded within the 30-day period of observation in all SBR tests. Co-metabolism did not appear to occur after acclimating the culture to petrodiesel in chemostat B80. This supports the observation that any sulfate concentration decrease in the B50 treatment with both cultures was due to the biodegradation of the biodiesel fraction, the FAMES compound in the oil blends.

3.2. FAMES degradation

The basic steps involved in the overall anaerobic degradation of waste are: (Aeckersberg et al., 1998): hydrolysis (Abumrad et al., 1984), acidogenesis and (Aktas et al., 2010) anaerobic oxidation. For biodiesel, which is composed of a mixture of FAMES, the first step is ester hydrolysis to their corresponding long-chain fatty acids (LCFAs) and methanol. C18:1-ME and C18:2-ME, the two highest concentration compounds in soybean biodiesel, are hydrolyzed to oleic acid (C18:1) and linoleic acid (C18:2). The initial concentrations of each FAMES in B100 were 21.3 ± 0.0 mg/L C16:0-ME, 8.0 ± 0.1 mg/L C18:0-ME, 48.4 ± 0.4 mg/L C18:1-ME, 121.7 ± 0.9 mg/L C18:2-ME, and 13.0 ± 0.1 mg/L C18:3-ME. When B100 was biodegraded using the culture pre-acclimated to B100 (circle symbols in Fig. 2), a 1-day lag phase was observed for C16:0-ME, C18:0-ME and C18:1-ME. Many studies have shown that high concentrations of LCFAs could cause microbial inhibition (Zonta et al., 2013). Lalman and Bagley, 2001, Lalman, and Bagley, 2002 reported that C18:1 concentrations above 30 mg/L inhibited acetate degradation while stearic acid (C18:0) up to 100 mg/L did not inhibit acetoclastic methanogenesis, and C18:2 above 100 mg/l inhibited butyrate degradation. Sousa et al. (2013) found that unsaturated C18:1 had a more inhibitory effect on methanogens than saturated C16:0 and C18:0. The inhibitory effect of LCFAs might be the reason for the observed lag phase at the beginning of the biodegradation process. The biodegradation of FAMES was estimated by nonlinear least-squares regression by fitting the concentration of the FAMES degraded (M_t) in the time (t) to exponential decay model using equation (Abumrad et al., 1984), $M_t = M_0 \times e^{-kt}$ (2)

Where M_t is the concentration at time t , M_0 is the initial concentration at time zero and k is the pseudo first-order constant. The pseudo first-order rate constant k did not incorporate the concentration of sulfate-reducing bacteria in the inoculum in this study. For those compounds having a lag phase, that initial time was excluded from the fitting of the data to the first-order kinetic model. The pseudo first-order rate constants for each individual FAME compound are shown in Table 1.

The first-order rate constant for the biodegradation of C18:1 was not significantly lower than those for all the other compounds ($p = 0.434$). The extent of removal for all the FAMES was 99% at the end of the experiment (day 19) as shown in Table 2 (column 3).

Similar findings were observed for the biodegradation of B100 using culture B80 (triangle symbols in Fig. 2), and, in this case, the lag-phase lasted two days for C16:0-ME, C18:0-ME and C18:1-ME. The first-order biodegradation rate constant was determined for each compound after excluding the lag-phase, and the resulting values are shown in Table 1. Compared to the same oil treated using culture B100, the first-order biodegradation rate constants for each FAMES decreased by 46% for C16:0-ME, 45% for C18:0-ME, 43% for C18:1-ME, 49% for C18:2-ME, and 47% for C18:3-ME. However, the removal extent was decreased to approximately 91% for all the FAMES at the end of the experiment, compared to 99% when the culture B100 was used.

When B50 was biodegraded using culture B100 (circle symbols in Fig. 3), no lag phase was observed for all compounds, probably because the initial concentration of the FAMES in B50 was half the concentration in B100. The initial concentrations of C18:1-ME and C18:2-ME

in B50 were 23.4 ± 0.4 mg/L and 60.2 ± 1.1 mg/L respectively. The inhibitory effect from their hydrolyzed LCFAs was reduced compared to the B100 treatment when using the same culture. The microbial activity was not inhibited at the initial time when compared to the treatment of B50 using culture B80. The rate constants of B50 treated by culture B100 were significantly higher than that of B50 ($p = 0.016$) and B100 ($p = 0.0007$) treated by culture B80 as shown in Table 1. For saturated FAMES, the degradation rate of C16:0-ME was slightly higher than that of C18:0-ME. As for the unsaturated FAMES, the first-order biodegradation rate constant was highest for C18:3-ME and the biodegradation rate increased as the number of double bonds increased. The removal extent for each FAMES at the end of the experiment (day 30) is shown in Table 2. For C16:0-ME, C18:0-ME and C18:1-ME, the removal extent was above 95% and over 97% for C18:2-ME and C18:3-ME, respectively. Although the initial concentration of FAMES in B50 was lower than that in B100, after 19 days of incubations, the removal of FAMES in B50 were 93% for C16:0-ME, 94% for C18:0-ME, 94% for C18:1-ME, 95% for C18:2-ME and 97% for C18:3-ME. In comparison, all the FAMES in B100 were depleted by more than 98% after the same period of incubation. The decrease of the removal extent of FAMES in the B50 treatment compared to B100 treatment by the same culture was probably due to the inhibitory effect from the petrodiesel fraction of B50 blends.

The biodegradation of B50 using culture B80 (triangle symbols in Fig. 3) revealed a 3-day lag phase for C18:0 and a 3-day slow degradation phase for all the other FAMES. This may be attributed to the fact that the culture, in this case, was exposed to elevated levels of petrodiesel. When compared to the same oil blends treatment by culture B100, the first-order biodegradation rate for each FAME in the B50 treatment by culture B80 were decreased by 54% for C16:0-ME, 50% for C18:0-ME, 62% for C18:1-ME, 61% for C18:2-ME and 52% for C18:3-ME (Table 1), or an average for all FAMES of 56%. The removal extent was decreased to around 80% of that by culture B100 (Table 2). Overall, the data collected in this study suggests that the first-order rate constants for the biodegradation of FAMES decreased with increases in the carbon chain length of saturated FAMES and increased with the increasing number of double bonds for unsaturated FAMES. These results are opposite to the biodegradation order trends observed in a previous study under aerobic conditions (Yassine et al., 2013). Degradation of fatty acids begins by the physical transport of long-chain fatty acids into the microbial cell. Some researchers have concluded that fatty acid uptake is a facilitated process (Abumrad et al., 1984, Nunn, 1986, Zhou et al., 1992) while others argued that fatty acids pass through the cell membrane by passive diffusion (Kohlwein and Paltauf, 1984, Noy, 1986, Cooper et al., 1987). The passive diffusion for fatty acid uptake is by direct diffusion not involving any carrier proteins. It operates when high concentrations of free fatty acids are being used as substrates (Ratledge, 1984). The long-chain hydrophobic hydrocarbons have low solubility in water. However, the presence of the carboxylate ester group and the double bonds enable the FAME molecules to form hydrogen bonds with water, which makes them more bioavailable. For the same carbon chain length, the solubility increased with the increase in the number of double bonds. The substrate bioavailability for microorganisms refers to the soluble substrate in the water. The reported solubility limits for the saturated C16:0-ME and C18:0-ME are 4 $\mu\text{g/L}$ and 0.2 $\mu\text{g/L}$, respectively, and unsaturated C18:1-ME, C18:2-ME and C18:3-ME are 3.7 $\mu\text{g/L}$, 21 $\mu\text{g/L}$ and 91 $\mu\text{g/L}$,

respectively (Krop et al., 1997). For unsaturated FAMES, the biodegradation rate increased with increases in the number of double bonds. This correlates well with their aqueous solubility due to the bioavailability of the substrate. FAMES partitioning test data from our lab (Wu et al., 2015) revealed that the soluble concentrations of FAMES in water were 25 µg/L for C16:0-ME, 7.9 µg/L for C18:0-ME, 42 µg/L for C18:1-ME, 84 µg/L for C18:2-ME, and 6.7 µg/L for C18:3-ME. All the FAMES except C18:3-ME showed a similar trend as reported. C18:3-ME with three double bonds is mostly unstable and more easily autoxidized (Frankel et al., 1981). This may have occurred during the partitioning test where, after sacrificing a set of samples, they were allowed to settle for 3 h under ambient conditions before the samples were further processed. If the FAMES mass transfer through the cell membrane is idealized according to the Fick's First Law of Diffusion, then the unsaturated FAMES, such as C18:3-ME, which have the highest solubility, would have a higher diffusion driving force across the cell membrane compared to the other FAMES. For the saturated FAMES, in addition to the faster mass transfer kinetics across the cell membrane, such as for C16:0 or C18:0, less energy would be required during metabolism inside the cell. Aktas et al. (2010) studied the intermediates of anaerobic biodegradation of biodiesel and found that the anaerobic biodegradation of saturated FAMES undergo a β -oxidation pathway in which the fatty acid intermediates are shortened by removal of two carbon fragments from the carboxyl end of the molecule to form a progressively shorter series of lower molecular-weight compounds. For example, the saturated C18:0-ME is first hydrolyzed to its fatty acid product octadecanoic acid (C18:0), then degraded to hexadecanoic acid (C16:0) by beta-oxidation. The saturated C16:0-ME, which has two fewer carbons in its carbon chain, is directly hydrolyzed to hexadecanoic acid (C16:0). However, faster mass transfer kinetics of the unsaturated FAMES across the cell membrane might be countered by slower enzymatic metabolism inside the cell due to the initial requirement to hydrolyze the double bonds prior to β -oxidation. The β -oxidation pathway can proceed only if a metabolic blockage has been eliminated, such as hydrolysis of a double bond. The more numerous the double bonds within the molecule, the more energy is required to enzymatically hydrolyze those bonds before β -oxidation can proceed (Ratledge, 1984). In the facilitated diffusion process, the transport of long-chain fatty acids across the membrane requires the presence of specific transport proteins and is an energy-mediated process. The presence of such proteins correlates with the cell's fatty acid binding activity (Ratledge, 1984). The *fadL* gene encodes membrane protein functions as transporters of long-chain fatty acids across the cell membrane. It contains many hydrophobic pockets and binding domains (Van Den Berg et al., 2004), and the substrate binding affinity increases with the increase of the hydrophobicity of the molecules (Black, 1990, Kunau et al., 1995, Van Den Berg et al., 2004). This is consistent with the degradation order trend of FAMES under aerobic conditions (Yassine et al., 2013), but contrary to the findings in this study under anaerobic conditions. Both processes lead to the direct entry of fatty acids into the cell, but result in a different trend in biodegradation order due to the different transport and biodegradation mechanisms discussed above.

3.3. Alkanes degradation

No biodegradation of total alkanes (nC10-nC22) in B0 and B50 was observed within the 30 days of observation as shown in Fig. 4. The result confirmed that the decrease of sulfate in

B50 blends was used for FAMES degradation only, not hydrocarbon degradation. The total alkane concentration using the B80 culture treatment was higher than that in B100 because the alkanes did not degrade in the chemostat of reactor B80. Alkanes, as a group of low chemical reactivity compound, are only degraded by certain microbial cultures such as strain TD 3 and strain Hxd3, and their metabolism requires specific enzymes and a sufficient exposure time to become a microbial substrate (Rueter et al., 1994, Heider et al., 1998, Wentzel et al., 2007). Study has shown that synthesis of new proteins is necessary in fatty acid grown cells in order to gain the ability to metabolized alkanes (Aeckersberg et al., 1998).

4. Conclusion

Results from this study indicate that biodiesel was effectively degraded, whereas petrodiesel resisted biodegradation under sulfate-reducing conditions. The degradation rate of individual FAMES decreased with an increase in the carbon chain length for saturated FAMES, and increased with an increasing number of double bonds for unsaturated FAMES. When blended with petrodiesel, the biodegradation of FAMES in biodiesel may be affected by: (Aeckersberg et al., 1998): the bioavailability of specific FAME compounds when they are transferred into the cell membrane (Abumrad et al., 1984); the lag-phase caused by the inhibition of the hydrolysis product of fatty acids (Aktas et al., 2010); previous exposure to petrodiesel due to the toxicity of petrodiesel.

Supplementary Material

Refer to Web version on PubMed Central for supplementary material.

Acknowledgment

Funding of this research was made possible through the U.S. Environmental Protection Agency (U.S. EPA) Oil Spill Research Program managed by the Land Remediation and Pollution Control Division of the National Risk Management Research Laboratory, Cincinnati, OH, under Contract No. EP-C-11-006, Work Assignment 3-19.

References

- Aeckersberg et al., 1998 Aeckersberg F, Rainey FA, Widdel F Growth, natural relationships, cell fatty acids and metabolic adaptation of sulfate-reducing bacteria utilizing long-chain alkanes under anoxic conditions *Archives Microbiol.*, 170 (5) (1998), pp. 361-369
- Abumrad et al., 1984 Abumrad NA, Park JH, Park CR Permeation of long-chain fatty acid into adipocytes. Kinetics, specificity, and evidence for involvement of a membrane protein *J. Biol. Chem.*, 259 (14) (1984), pp. 8945-8953 [PubMed: 6746632]
- Aktas et al., 2010 Aktas DF, Lee JS, Little BJ, Ray RI, Davidova IA, Lyles CN, Suflita JM Anaerobic metabolism of biodiesel and its impact on metal corrosion *Energy Fuels*, 24 (5) (2010), pp. 2924-2928
- Black, 1990 Black PN Characterization of FadL-specific fatty acid binding in *Escherichia coli* *Biochim. Biophys. Acta (BBA)/Lipids Lipid Metabol.*, 1046 (1) (1990), pp. 97-105
- Boopathy, 2004 Boopathy R Anaerobic biodegradation of no. 2 petrodiesel fuel in soil: a soil column study *Bioresour. Technol.*, 94 (2) (2004), pp. 143-151 [PubMed: 15158506]
- Cooper et al., 1987 Cooper R, Noy N, Zakim D A physical-chemical model for cellular uptake of fatty acids: prediction of intracellular pool sizes *Biochemistry*, 26 (18) (1987), pp. 5890-5896 [PubMed: 3676296]

- DeMello et al., 2007 DeMello JA, Carmichael CA, Peacock EE, Nelson RK, Samuel Arey J, Reddy CM Biodegradation and environmental behavior of biodiesel mixtures in the sea: an initial study *Mar. Pollut. Bull.*, 54 (7) (2007), pp. 894–904 [PubMed: 17481669]
- Frankel et al., 1981 Frankel E, Neff W, Selke E Analysis of autoxidized fats by gas chromatography-mass spectrometry: VII. Volatile thermal decomposition products of pure hydroperoxides from autoxidized and photosensitized oxidized methyl oleate, linoleate and linolenate *Lipids*, 16 (5) (1981), pp. 279–285
- Gupta et al., 1996 Gupta M, Sharma D, Suidan MT, Sayles GD Biotransformation rates of chloroform under anaerobic conditions – I Methanogenesis. *Water Res.*, 30 (6) (1996), pp. 1377–1385
- Heider et al., 1998 Heider J, Spormann AM, Beller HR, Widdel F Anaerobic bacterial metabolism of hydrocarbons *FEMS Microbiol. Rev.*, 22 (5) (1998), pp. 459–473
- Kohlwein and Paltauf, 1984 Kohlwein SD, Paltauf F Uptake of fatty acids by the yeasts, *Saccharomyces uvarum* and *Saccharomycopsis lipolytica* *Biochim. Biophys. Acta (BBA)/Lipids Lipid Metabo.*, 792 (3) (1984), pp. 310–317
- Krop et al., 1997 Krop HB, Van Velzen MJM, Parsons JR, Govers HAJ n-Octanol-water partition coefficients, aqueous solubilities and Henry's law constants of fatty acid esters *Chemosphere*, 34 (xxx) (1997), pp. 107–119
- Kunau et al., 1995 Kunau W-H, Dommies V, Schulz H β -oxidation of fatty acids in mitochondria, peroxisomes, and bacteria: a century of continued progress *Prog. Lipid Res.*, 34 (4) (1995), pp. 267–342 [PubMed: 8685242]
- Lalman and Bagley, 2001 Lalman JA, Bagley DM Anaerobic degradation and methanogenic inhibitory effects of oleic and stearic acids *Water Res.*, 35 (12) (2001), pp. 2975–2983 [PubMed: 11471698]
- Lalman, and Bagley, 2002 Lalman JA, Bagley DM Effects of C18 long chain fatty acids on glucose, butyrate and hydrogen degradation *Water Res.*, 36 (13) (2002), pp. 3307–3313 [PubMed: 12188129]
- Maillacheruvu et al., 1993 Maillacheruvu KY, Parkin GF, Peng CY, Kuo W, Oonge ZI, Lebduschka V Sulfide toxicity in anaerobic systems fed sulfate and various organics *Water Environ. Res.*, 65 (2) (1993), pp. 100–109
- Miller and Mudge., 1997 Miller NJ, Mudge SM The effect of biodiesel on the rate of removal and weathering characteristics of crude oil within artificial sand columns *Spill Sci. Technol. Bull.*, 4 (1) (1997), pp. 17–33
- Mukherji. et al., 2004 Mukherji S, Jagadevan S, Mohopatra G, Vijay A Biodegradation of petrodiesel oil by an Arabian sea sediment culture isolated from the vicinity of an oil field *Bioresour. Technol.*, 95 (3) (2004), pp. 281–286 [PubMed: 15288270]
- Noy, 1986 Noy N Physical-chemical model for the entry of water-insoluble compounds into cells. studies of fatty acid uptake by the liver *Biochemistry*, 25 (8) (1986), pp. 2013–2202 [PubMed: 3707927]
- Nunn, 1986 Nunn WD A molecular review of fatty acid catabolism in *Escherichia coli* *Microbiol. Rev.*, 50 (2) (1986), pp. 179–192 [PubMed: 3523188]
- Owsianiak et al., 2009 Owsianiak M, Chrzanowski L, Szulc A, Staniewski J, Olszanowski A, Olejnik-Schmidt AK, Heipieper HJ Biodegradation of petrodiesel/biodiesel blends by a consortium of hydrocarbon degraders: effect of the type of blend and the addition of biosurfactants *Bioresour. Technol.*, 100 (3) (2009), pp. 1497–1500 [PubMed: 18815027]
- Pareek et al., 2000 Pareek Sandeep, Azuma Jun-Ichi, Shimizu Yoshihisa, Matsui Saburo Hydrolysis of newspaper polysaccharides under sulfate reducing and methane producing conditions *Biodegradation*, 11 (4) (2000), pp. 229–237 [PubMed: 11432581]
- View Record in ScopusGoogle Scholar Pasqualino et al, 2006
- Pasqualino JC, Montane D, Salvado J Synergic effects of biodiesel in the biodegradability of fossil-derived fuels *Biomass Bioenergy*, 30 (10) (2006), pp. 874–879
- Rueter et al., 1994 Rueter P, Rabus R, Wilkes H, Aeckersberg F, Rainey FA, Jannasch HW, Widdel F Anaerobic oxidation of hydrocarbons in crude oil by new types of sulphate reducing bacteria *Nature*, 372 (6505) (1994), pp. 455–458 [PubMed: 7984238]
- Ratledge, 1984 Ratledge C microbial conversions of alkanes and fatty acids *J. Am. Oil Chem. Soc.*, 61 (2) (1984), pp. 447–453

- Sørensen et al., 2011 Sørensen G, Pedersen DV, Nørgaard AK, Sørensen KB, Nygaard SD Microbial growth studies in biodiesel blends *Bioresour. Technol*, 102 (8) (2011), pp. 5259–5264 [PubMed: 21376581]
- Sousa et al., 2013 Sousa DZ, Salvador AF, Ramos J, Guedes AP, Barbosa S, Stams AMS, Alves MM, Pereira MA Activity and viability of methanogens in anaerobic digestion of unsaturated and saturated long-chain fatty acids *Appl. Environ. Microbiol*, 79 (14) (2013), pp. 4239–4245 [PubMed: 23645196]
- Van Den Berget al., 2004 Van Den Berg B, Black PN, Clemons WM Jr., Rapoport TA Crystal structure of the long-chain fatty acid transporter FadL *Science*, 304 (5676) (2004), pp. 1506–1509 [PubMed: 15178802]
- Wentzel et al., 2007 Wentzel A, Ellingsen TE, Kotlar H, Zotchev SB, Throne-Holst M Bacterial metabolism of long-chain n-alkanes *Appl. Microbiol. Biotechnol*, 76 (6) (2007), pp. 1209–1221 [PubMed: 17673997]
- Widdel and Rabus, 2001 Widdel F, Rabus R Anaerobic biodegradation of saturated and aromatic hydrocarbons *Curr. Opin. Biotechnol*, 12 (3) (2001), pp. 259–276 [PubMed: 11404104]
- Wu et al., 2015 Wu S, Yassine MH, Suidan MT, Venosa AD Anaerobic biodegradation of soybean biodiesel and diesel blends under methanogenic conditions *Water Res.*, 87 (2015), pp. 395–402 [PubMed: 26454635]
- Yassine et al., 2012 Yassine MH, Wu S, Suidan MT, Venosa AD Microtox aquatic toxicity of petrodiesel and biodiesel blends: the role of biodiesel's autoxidation products *Environ. Toxicol. Chem*, 31 (12) (2012), pp. 2757–2762 [PubMed: 22949027]
- Yassine et al., 2013 Yassine MH, Wu S, Suidan MT, Venosa AD Aerobic biodegradation kinetics and mineralization of six petrodiesel/soybean-biodiesel blends *Environ. Sci. Technol*, 47 (9) (2013), pp. 4619–4627 [PubMed: 23550844]
- Zhang et al., 1998 Zhang X, Peterson C, Reece D, Haws R, Möller G Biodegradability of biodiesel in the aquatic environment *Trans. Am. Soc. Agric. Eng*, 41 (5) (1998), pp. 1423–1430
- Zhou et al., 1992 Zhou S-L, Stump D, Sorrentino D, Potter BJ, Berk PD Adipocyte differentiation of 3T3-L1 cells involves augmented expression of a 43-kDa plasma membrane fatty acid-binding protein *J. Biol. Chem*, 267 (20) (1992), pp. 14456–14461 [PubMed: 1629231]
- Zonta et al., 2013 Zonta T, Alves MM, Flotats X, Palatsi J Modelling inhibitory effects of long chain fatty acids in the anaerobic digestion process *Water Res.*, 47 (3) (2013), pp. 1369–1380 [PubMed: 23276428]

Highlights

- Sulfate-reducing biodegradation of biodiesel and diesel blends were characterized.
- Saturated FAME: degradation rate decreased with an increasing carbon chain length.
- Unsaturated FAME: degradation rate increased with an increasing double bonds.
- Degradation rate was affected by the bioavailability of FAMES in aquatic system.
- Degradation rate was affected by the inhibition of long-chain fatty acids.

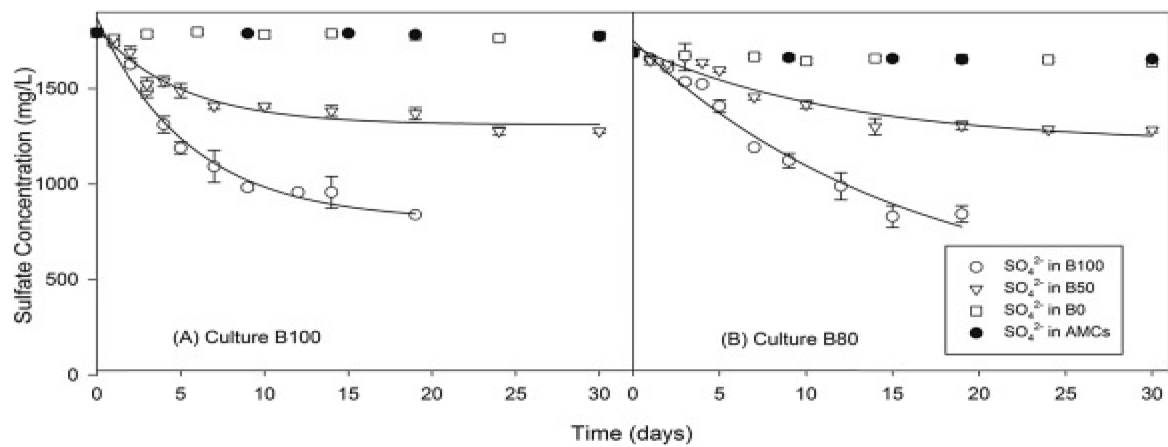


Figure 1.
Sulfate utilization with the culture from reactor B100 (A) and reactor B80 (B).

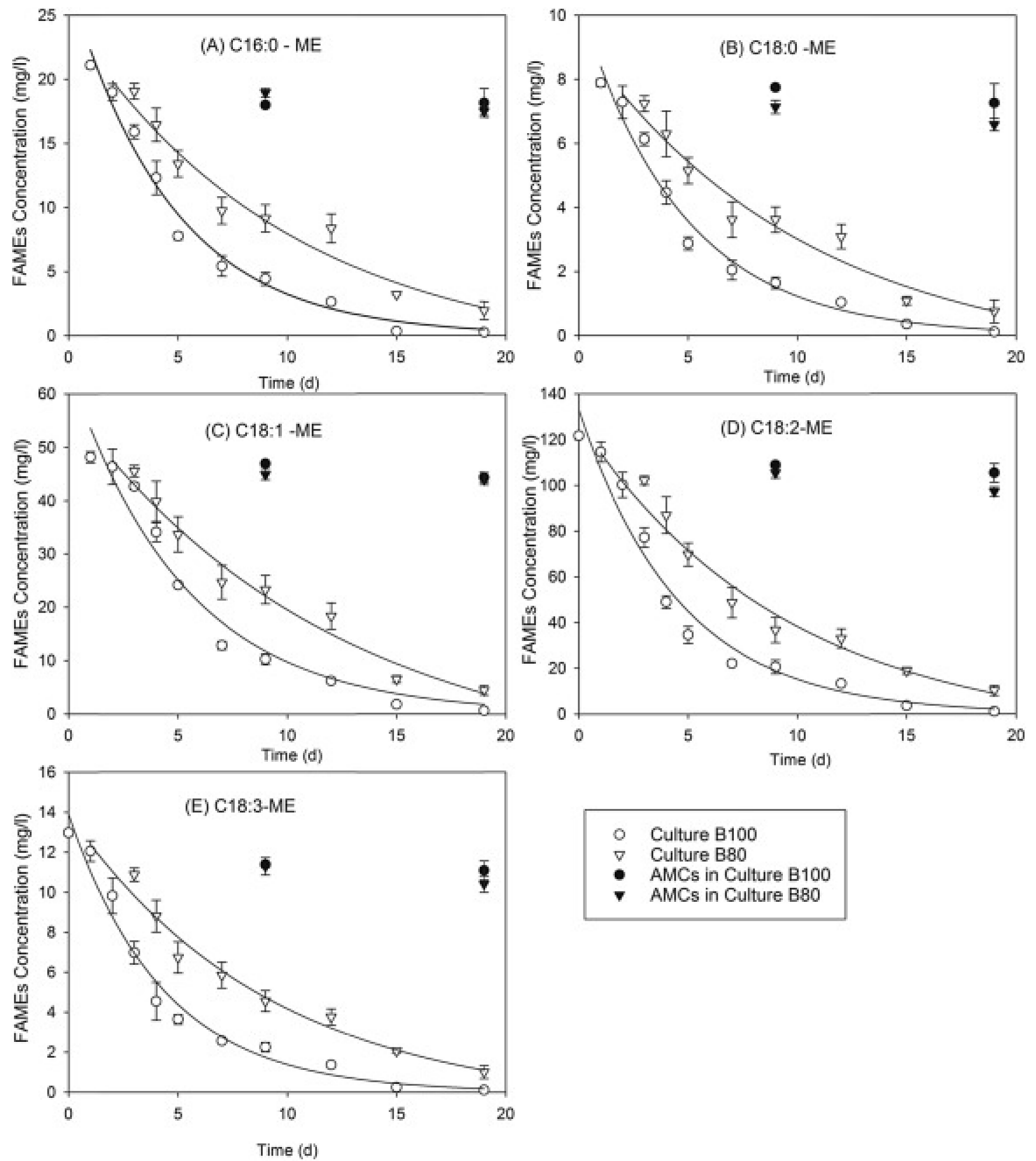


Figure 2. Biodegradation of FAMES in B100 treatment. The circle symbols are for the culture from reactor B100. The triangle symbols are for the culture from reactor B80. The blank symbols are KCs.

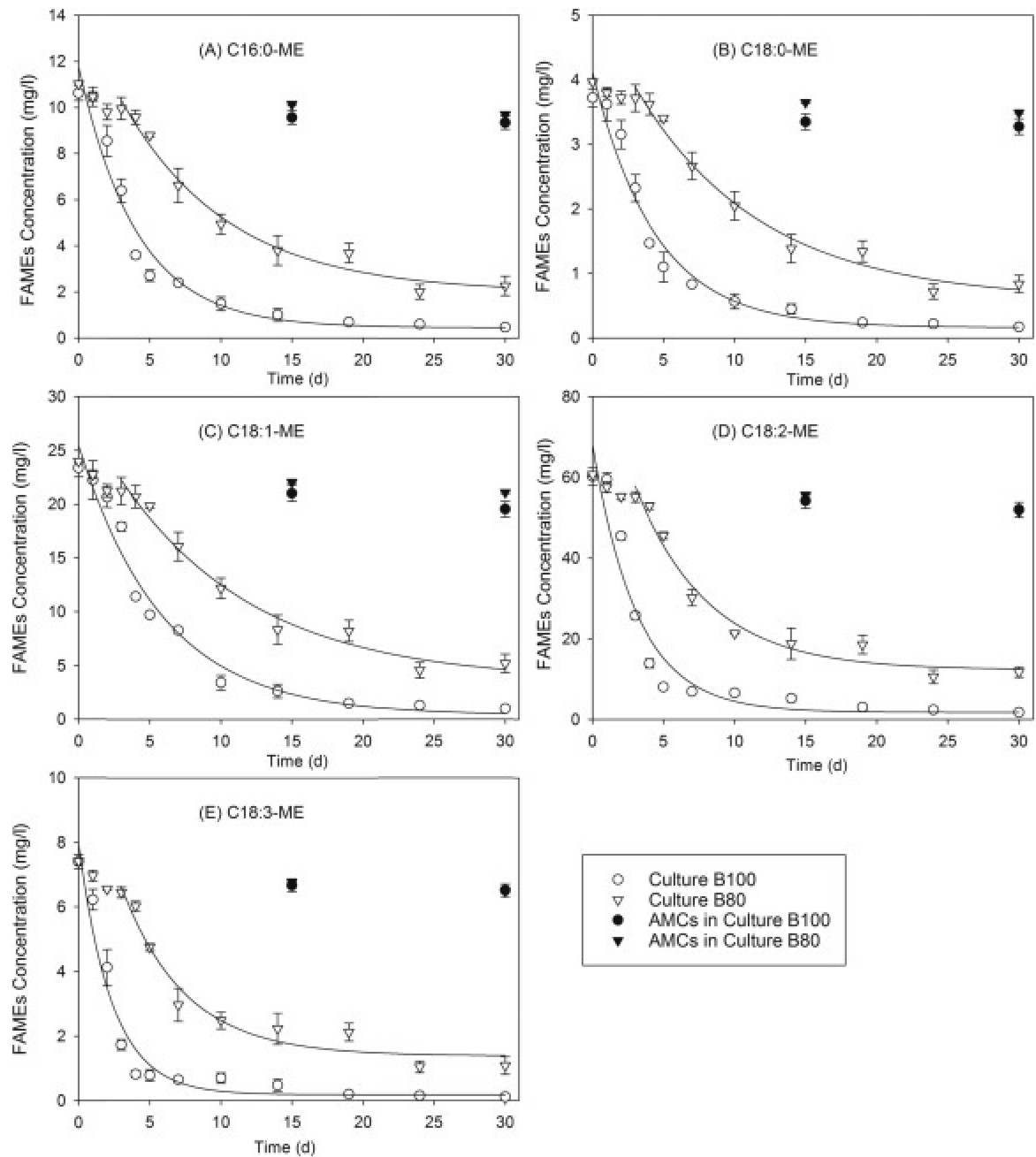


Figure 3. Biodegradation of FAMES in B50 treatment. The circle symbols are for the culture from reactor B100. The triangle symbols are for the culture from reactor B80. The blank symbols are KCs.

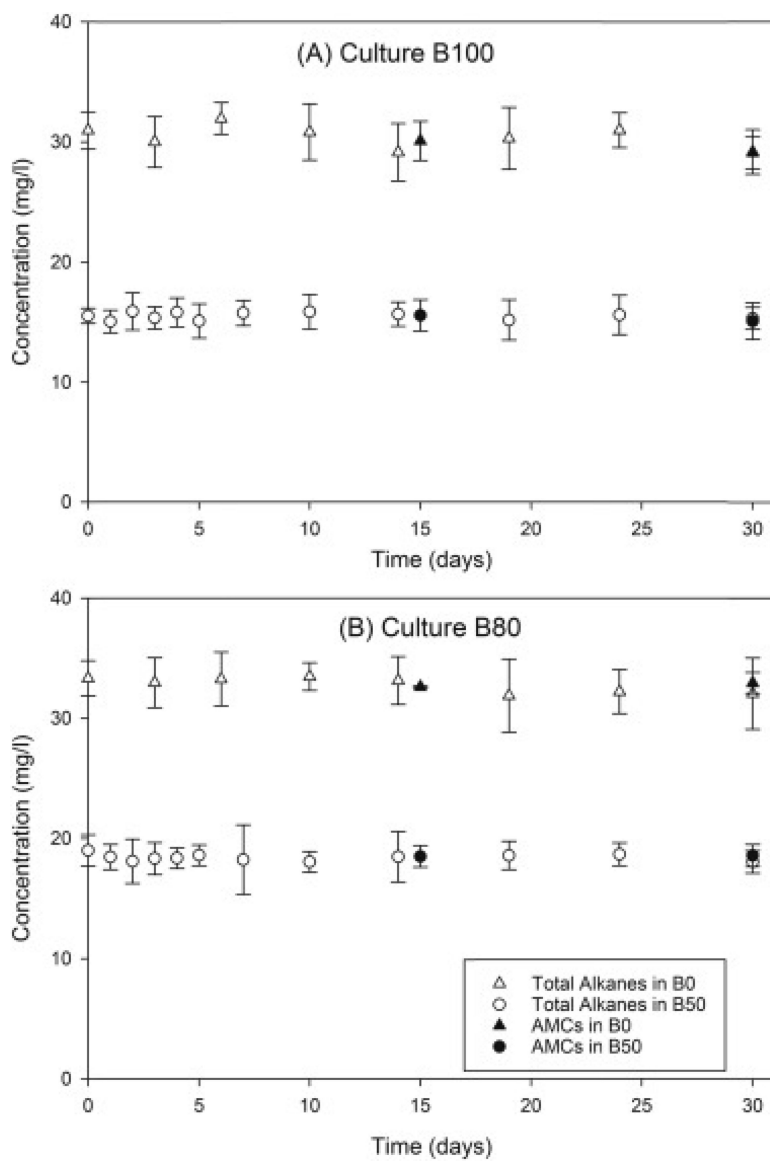


Figure 4. Total alkanes (nC10 to nC22) degradation with the culture from reactor B100 (A) and reactor B80 (B).

Table 1.

Pseudo-first order biodegradation rate constants for FAMES in B100 and B50 treated by culture from reactor B100 and B80 (d⁻¹).

	FAMES in B100		FAMES in B50	
	Culture B100	Culture B80	Culture B100	Culture B80
C16:0-ME	0.215 ± 0.017	0.100 ± 0.038	0.246 ± 0.039	0.134 ± 0.023
C18:0-ME	0.214 ± 0.018	0.097 ± 0.038	0.227 ± 0.035	0.113 ± 0.020
C18:1-ME	0.189 ± 0.020	0.082 ± 0.029	0.170 ± 0.026	0.105 ± 0.021
C18:2-ME	0.215 ± 0.021	0.105 ± 0.032	0.319 ± 0.060	0.196 ± 0.037
C18:3-ME	0.230 ± 0.021	0.109 ± 0.028	0.427 ± 0.064	0.224 ± 0.051

Table 2.

Initial concentration of FAMES and the removal extent of FAMES in B100 and B50 treated by culture from reactor B100 and B80.

Compounds	FAMES in B100			FAMES in B50		
	Initial concentration (mg/L)	Treated by culture B100 (%)	Treated by culture B80 (%)	Initial concentration (mg/L)	Treated by culture B100 (%)	Treated by culture B80 (%)
C16:0-ME	21.3 ± 0.1	99	91	10.6 ± 0.3	96	79
C18:0-ME	8.0 ± 0.1	99	91	3.7 ± 0.1	95	79
C18:1-ME	48.4 ± 0.4	99	91	23.8 ± 0.4	96	78
C18:2-ME	121.7 ± 0.9	99	91	60.2 ± 1.1	97	81
C18:3-ME	13.0 ± 0.1	99	92	7.4 ± 0.2	99	85